Preparation and Characterization of Polypyrrole–Tin(IV) Oxide Nanocomposite Colloids

Shuichi Maeda and Steven P. Armes*

School of Chemistry and Molecular Sciences, University of Sussex, Falmer, Brighton, BN1 9QJ, U.K.

Received July 18, 1994. Revised Manuscript Received September 22, 1994®

Recently we described the synthesis of polypyrrole–silica nanocomposite colloids using ultrafine silica particles as particulate dispersants. In the present study we have chemically polymerized pyrrole in the presence of various other ultrafine inorganic oxide sols such as tin(IV) oxide, zirconia, antimony(V) oxide, yttria, and titanium(IV) oxide. We find that only the tin(IV) oxide sols act as effective particulate dispersants; the other four oxide systems failed to prevent macroscopic precipitation of the polypyrrole. The resulting polypyrrole–tin(IV) oxide nanocomposite colloids have been extensively characterized in terms of their chemical composition, particle size, morphology, surface composition, colloidal stability, and electroactivity. These polypyrrole–tin(IV) oxide particles have a rather polydisperse "raspberry" morphology compared to the relatively monodisperse "raspberry" morphologies found for polypyrrole–silica particles. Increasing the initial concentration of the tin(IV) oxide sol leads to lower levels of conducting polymer being incorporated into the nanocomposite particles. The high density of the tin(IV) oxide particles leads to polypyrrole–tin(IV) oxide nanocomposites with significantly higher particle densities than the polypyrrole–silica nanocomposites. Our X-ray photoelectron spectroscopy studies confirm that the polypyrrole–tin(IV) oxide particles are surface-rich with respect to the tin(IV) oxide component. These nanocomposites are not as stable as the polypyrrole–silica colloids with respect to pH-induced aggregation, but their solid-state conductivities are higher by up to an order of magnitude. The highest conductivity obtained for these polypyrrole–tin(IV) oxide nanocomposites in the present study is 23 S cm^{-1}.

Introduction

Polypyrrole is a relatively air-stable electrically conductive polymer.[1–3] It is normally chemically synthesized as an intractable and unprocessable bulk powder precipitate.[4,5] The poor processability of polypyrrole has been improved by the synthesis of β-substituted derivatives which are soluble in a variety of common solvents.[6–8] However, the β-substituted monomer precursors are often tedious to synthesize, making large-scale production uneconomical. In addition, the solubility of such derivatives is limited, particularly in the doped form.

An alternative approach is the preparation of sterically stabilised polypyrrole colloids via dispersion polymerization. Since 1986 various research groups have described the preparation of sterically stabilized colloidal dispersions of polypyrrole using either commercial polymers such as methyl cellulose,[9,10] poly(ethylene oxide),[11–14] poly(vinylpyrrolidone),[12,13,15] poly(vinylpyridine),[16,17] and poly(vinyl alcohol)[10,13,15,18] or tailor-made copolymers such as poly(2-vinylpyridine-*co*-*n*-butyl methacrylate)[19] and poly(2-(dimethylamino)ethyl methacrylate-*b*-*n*-butyl methacrylate).[20] Thin conductive films can be easily fabricated from such dispersions, thus this approach significantly improves the processability of these otherwise intractable materials.

There have been numerous publications describing the preparation of inorganic–organic hybrid materials which contain polypyrrole as the organic component. For example, Partch et al. have recently described the preparation of several polypyrrole-coated inorganic oxide composites by utilising the inorganic oxide as a

* To whom correspondence should be addressed.

® Abstract published in *Advance ACS Abstracts,* November 1, 1994.

(1) Kanazawa, K. K.; Diaz, A. F.; Geiss, R. H.; Gill, W. D.; Kwak, J. F.; Logan, J. A.; Rabolt, J. F.; Street, G. B. *J. Chem. Soc., Chem. Commun.* **1979**, 854.
(2) Diaz, A. F.; Kanazawa, K. K. In *Extended Linear Chain Compounds*; Miller, J. S., Ed.; Plenum Press: London, 1983; Vol 3, p 417.
(3) Street, G. B. In *Handbook of Conducting Polymers*; Skotheim, T. A., Ed., Dekker, New York, 1985; Vol. 1, p 265.
(4) Myers, R. E. *J. Electron. Mater.* **1986**, *15*(2), 61.
(5) Rapi, S.; Bocchi, V.; Gardini, G. P. *Synth. Met.* **1988**, *24*, 217.
(6) Bryce, M. R.; Chissel, A.; Kathirgamanathan, P.; Parker, D.; Smith, N. R. M. *J. Chem. Soc., Chem. Commun.* **1987**, 466.
(7) Ezquerra, T. A.; Ruhe, J.; Wegner, G. *Chem. Phys. Lett.* **1988**, *194*, 194.
(8) Merz, A.; Schwarz, R.; Schropp, R. *Adv. Mater.* **1992**, *4*, 409.
(9) Bjorklund, R. B.; Liedberg, B. *J. Chem. Soc., Chem. Commun.* **1986**, 1293.
(10) Epron, F.; Henry, F.; Sagnes, O. *Makromol. Chem., Macromol. Symp.* **1990**, *35/36*, 527.
(11) Cawdery, N.; Obey, T. M.; Vincent, B. *J. Chem. Soc., Chem. Commun.* **1988**, 1189.
(12) Markham, G.; Obey, T. M.; Vincent, B. *Colloids Surf.* **1990**, *51*, 239.
(13) Armes, S. P.; Aldissi, M.; Idzorek, G. C.; Keaton, P. W.; Rowton, L. J.; Stradling, G. L.; Collopy, M. T.; McColl, D. B. *J. Colloid Interface Sci.* **1991**, *141*, 119.
(14) Odegard, R.; Skotheim, T. A.; Lee, H. S. *J. Electrochem. Soc.* **1991**, *138*, 2930.
(15) Armes, S. P.; Vincent, B. *J. Chem. Soc., Chem. Commun.* **1987**, 288.
(16) Armes, S. P.; Aldissi, M.; Agnew, S. F. *Synth. Met.* **1989**, *28*, C837.
(17) Rawi, Z.; Mykytiuk, J.; Armes, S. P. *Colloids Surf.* **1992**, *68*, 215.
(18) Armes, S. P.; Miller, J. F.; Vincent, B. *J. Colloid Interface Sci.* **1987**, *118*, 410.
(19) Armes, S. P.; Aldissi, M. *Polymer* **1990**, *31*, 569.
(20) Beadle, P. M.; Rowan, L.; Mykytiuk, J.; Billingham, N. C.; Armes, S. P. *Polymer* **1993**, *34*, 1561.

0897-4756/95/2807-0171$09.00/0

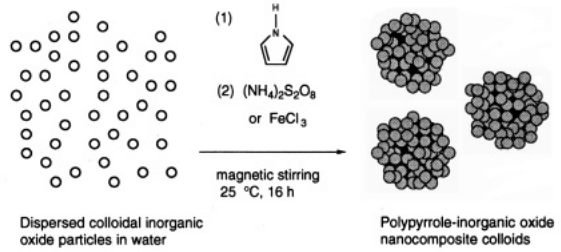

Figure 1. Schematic formation of polypyrrole–inorganic oxide nanocomposite colloids from the original inorganic oxide particles.

colloidal oxidant.[21] Mehrotra *et al.* have synthesized polypyrrole–silica "hybrid glasses" by the in situ chemical polymerization of pyrrole in a host glass matrix containing copper ions.[22] Yoneyama and co-workers have incorporated a wide range of particulate inorganic oxides such as titanium(IV) oxide, tungsten(VI) oxide, and manganese(IV) oxide[23,24] into electrochemically synthesised thin films of polypyrrole. In addition, Yamamoto's group have synthesized organic–organic hybrid particles which are apparently colloidally stable by polymerizing pyrrole onto the surface of poly(styrene-*co*-butadiene) latexes.[25]

Recently we have reported the preparation and characterization of novel polypyrrole–silica nanocomposite colloids using small silica particles as a particulate dispersant.[26–29] In this approach the silica particles act as a high surface area colloidal substrate for the precipitating polypyrrole, and the resulting nanocomposites are made up of microaggregates of the original silica particles "glued" together by the polypyrrole component, which gives rise to a distinctive "raspberry" particle morphology (see Figure 1). We found that, for 20 nm diameter silica particles, an initial silica concentration of approximately 1.0 w/v % was required for the quantitative formation of stable colloidal dispersions of polypyrrole–silica particles. Both the initial silica concentration and the choice of the chemical oxidant ($(NH_4)_2S_2O_8$ or $FeCl_3$) can significantly affect both the particle size and polypyrrole content of these nanocomposites. Their solid-state pressed pellet conductivities are consistently lower by 1–3 orders of magnitude relative to bulk powders prepared under the same conditions. However, the addition of sodium *p*-tosylate to these colloid syntheses can enhance these conductivities by at least an order of magnitude. Furthermore, given their good colloid stabilility with respect to pH-induced aggregation and their potentially facile surface functionalization,[28] we believe that these polypyrrole–silica nanocomposites will have interesting biological applications (*e.g.*, as highly colored "marker" particles in visual agglutination immunodiagnostic assays[30]).

In the present work we have investigated the potential use of other commercial inorganic oxide colloidal particles as alternative particulate dispersants for polypyrrole. In particular, we have examined the following novel oxide systems: tin(IV) oxide, zirconia, antimony(V) oxide, yttria, and titanium(IV) oxide.

Experimental Section

Inorganic Oxide Characterization. In our initial nanocomposite syntheses our surface area calculations were based on the manufacturer's particle size data and density literature values for each of the five inorganic oxide colloids. In our later work the absolute densities of the pristine and doped tin(IV) oxide sol (SN-15 and DP-5730A; both Nyacol Products) were accurately determined by helium pycnometry (Micromeritics Accupyc 1330 or QuantaChrome Ultrapyc instrument) to be 4.77 and 4.34 g cm^{-3}, respectively. These values are significantly lower than the "macroscopic" density of 6.95 g cm^{-3} normally quoted for tin(IV) oxide. This is presumably due to the rather small particle size (and hence relatively high content of surface-adsorbed water) of these sols (see Results and Discussion). The average particle size of these two sols were calculated using the above density values together with BET data (nitrogen adsorbate) obtained using either a Micromeritics Gemini 2360 or a QuantaChrome Nova 1000 instrument. These latter measurements were carried out on approximately 100–200 mg of both the pristine and doped tin(IV) oxide sols and also on a similar quantity of 20 nm silica sol (each of these dried powder samples were obtained by freeze-drying the respective aqueous dispersions). The specific surface area values cited are an average of at least two BET runs and have an experimental error of approximately ±5%. [It was found that further drying of these samples at elevated temperature had different effects on their specific surface area. Thus the surface area of silica samples dried at 120 °C for several hours increased slightly from 165 to 174 $m^2 g^{-1}$ due to the loss of adsorbed water. On the other hand, the surface area of the pristine tin(IV) oxide sol dried from its aqueous dispersion at 70 °C in air overnight decreased by more than a factor of 6 relative to the same freeze-dried material, presumably due to particle sintering].

Colloid Syntheses. The general preparation of the polypyrrole–silica nanocomposite colloids has been described in detail in our earlier publications.[26–29] Essentially the same procedure was utilized for the polypyrrole–inorganic oxide nanocomposite colloids in the present study, except that the oxidant was added *last* to the reaction mixture. Thus, pyrrole (1.00 mL) was added to a colloidal dispersion containing 1.0–10.0 g (dry weight) of either silica, pristine tin(IV) oxide, antimony-doped tin(IV) oxide, zirconia, antimony(V) oxide, yttria (donated by Nyacol Products), or titanium(IV) oxide (donated by Tioxide Specialities) in 75 mL of deionized water at 25 °C with constant stirring. A solution of $(NH_4)_2S_2O_8$ (3.84 g) or $FeCl_3 \cdot 6H_2O$ (9.10 g) in 25 mL of deionized water was then added to this stirred solution (total solvent volume = 100 mL) and the solution turned black within 5 min. The polymerization was allowed to proceed for 16 h. All syntheses involving yttria, titanium(IV) oxide, zirconia, and antimony(V) oxide dispersions yielded only macroscopic black precipitates, i.e., essentially no colloid formation. No attempts were made to characterize these precipitates. The black colloidal dispersions obtained using the two tin(IV) oxide sols were centrifuged for 6000 rpm for 30 min using a Beckman J2-21 instrument and the resulting black sediments were redispersed in deionized water using an ultrasonic bath. In each case this centrifugation–redispersion cycle was repeated twice more in order to

(21) Partch, R.; Gangolli, S. G.; Matijevic, E.; Cai, W.; Arajs, S. *J. Colloid Interface Sci.* **1991**, *144*, 27.
(22) Mehrotra, V.; Keddie, J. L.; Miller, J. M.; Giannelis, E. P. *J. Non-Cryst. Solids* **1991**, *136*, 97.
(23) Kawai, K.; N. Mihara, N.; Kuwabata, S.; Yoneyama, H. *J. Electrochem. Soc.* **1990**, *137*, 1793.
(24) (a) Yoneyama, H.; Shoji, Y. *J. Electrochem. Soc.* **1990**, *137*, 3826. (b) Yoneyama, H.; Kishimoto, A.; Kuwabata, S. *J. Chem. Soc., Chem. Commun.* **1991**, 986.
(25) Liu, C.; Maruyama, T.; Yamamoto, T. *Polym. J.* **1993**, *25*, 363.
(26) Maeda, S.; Armes, S. P. *J. Colloid Interface Sci.* **1993**, *159*, 257.
(27) (a) Maeda, S.; Armes, S. P. *J. Mater. Chem.* **1994**, *4*, 935. (b) Flitton, R.; Johal, J.; Maeda, S.; Armes, S. P. Submitted to *J. Colloid Interface Sci.*
(28) Maeda, S.; Armes, S. P. *ACS Polym. Prepr.* **1994**, *35(1)*, 217.
(29) Armes, S. P.; Maeda, S.; Gill, M. *ACS PMSE* **1994**, *70(1)*, 352.
(30) Tarcha, P. J.; Misun, D.; Finley, D.; Wong, M.; Donovan, J. J. In *Polymer Latexes*; eds. Daniels, E. S., Sudol, E. D., El-Assar, M. S. Eds.; ACS Symp. Ser. No. 492; American Chemical Society: Washington, DC, 1992; Chapter 22, p 347.

Table 1. Evaluation of Various Commercial Colloidal Inorganic Oxides as Potential Particulate Dispersants for Polypyrrole

inorganic oxides	manufacturer	particle size[a] (nm)	initial concn (w/v %)	oxidant type	colloid formation ?
SiO_2	Nyacol Products	20	1.0–3.4	$FeCl_3{\cdot}6H_2O$	yes
SiO_2	Nyacol Products	20	1.0–3.4	$(NH_4)_2S_2O_8$	yes
SnO_2[b]	Nyacol Products	8	1.4–3.4	$FeCl_3{\cdot}6H_2O$	yes
SnO_2[b]	Nyacol Products	8	3.4–10.0	$(NH_4)_2S_2O_8$	no
SnO_2[c]	Nyacol Products	10	1.5–3.4	$FeCl_3{\cdot}6H_2O$	yes
SnO_2[c]	Nyacol Products	10	3.4–10.0	$(NH_4)_2S_2O_8$	no
TiO_2	Tioxide Specialities	18	3.4–10.0	$FeCl_3{\cdot}6H_2O$	no
TiO_2	Tioxide Specialities	18	3.4–10.0	$(NH_4)_2S_2O_8$	no
TiO_2	Tioxide Specialities	35	3.4–10.0	$FeCl_3{\cdot}6H_2O$	no
TiO_2	Tioxide Specialities	35	3.4–10.0	$(NH_4)_2S_2O_8$	no
Sb_2O_5	Nyacol Products	50	3.4–10.0	$FeCl_3{\cdot}6H_2O$	no
Sb_2O_5	Nyacol Products	50	3.4–10.0	$(NH_4)_2S_2O_8$	no
ZrO_2	Nyacol Products	5	3.4–10.0	$FeCl_3{\cdot}6H_2O$	no
ZrO_2	Nyacol Products	5	3.4–10.0	$(NH_4)_2S_2O_8$	no
Y_2O_3	Nyacol Products	5	3.4–10.0	$FeCl_3{\cdot}6H_2O$	no
Y_2O_3	Nyacol Products	5	3.4–10.0	$(NH_4)_2S_2O_8$	no

[a] As determined by transmission electron microscopy. [b] Pristine tin(IV) oxide (SN-15; 2.0×10^{-3} S cm^{-1}). [c] Antimony-doped tin(IV) oxide (DP-5730A; 7.6×10^{-2} S cm^{-1}).

completely remove the excess small tin(IV) oxide particles from the larger polypyrrole–tin(IV) oxide nanocomposite particles.

Colloid Characterization. *Chemical Composition and Conductivity.* The chemical composition of the polypyrrole–tin(IV) oxide nanocomposites was quantitatively determined using both elemental microanalyses (Perkin-Elmer 2400 instrument) and thermogravimetric analyses (Perkin-Elmer TGA-7 instrument; scan rate 40 °C/min in air). In the former method the carbon content of the dried nanocomposites was simply compared to the carbon content of the corresponding polypyrrole bulk powder synthesized in the absence of inorganic oxide particles (typically 56.0 ± 0.5%). In the latter method the nanocomposites were heated up to 800 °C and the observed mass loss was attributed to the quantitative pyrolysis of the conducting polymer. A small correction was made for the water content of the tin(IV) oxide sols when calculating the conducting polymer content of the nanocomposites.

Fourier transform infrared (F.T.I.R.) spectroscopy studies were carried out on samples dispersed in KBr disks using a Perkin-Elmer FTS-40 instrument (typically 100 scans/spectrum at 4 cm^{-1} resolution). Visible absorption spectra of polypyrrole–tin(IV) oxide dispersions diluted in buffer solutions in the pH range 3–12 were recorded using a UNICAM UV/vis spectrometer. All conductivity measurements were made on compressed pellets of dried powders using the conventional four-point probe technique at room temperature.

Particle Size and Colloidal Stability. The particle size and colloidal stability (with respect to pH-induced aggregation) of both the polypyrrole–tin(IV) oxide nanocomposites were examined by dispersing these particles into buffer solutions in the pH range 3–12 using a BI-DCP disk centrifuge photosedimentometer (Brookhaven Instruments Corp.) at 25 °C with an external density gradient[31] using the following procedure: the nanocomposite dispersions were first diluted to 0.1–0.5 w/v % by adding them to the buffer solutions in the pH range 3–12 containing 20 v/v % methanol. A total of 0.20 mL of each of the diluted solutions was injected via syringe into 15 mL of the corresponding buffered spin fluid which contained 1.0 mL of methanol to create the "density gradient" which leads to fractionation of the particles within the sample. The 6000–7000 rpm centrifugation rate corresponded to run times of approximately 10–20 min. To select an appropriate extinction coefficient correction factor, it was assumed that the highly absorbing polypyrrole–tin(IV) oxide particles have similar scattering characteristics to carbon black. The densities of these nanocomposites were calculated from the combined (elemental microanalyses and thermogravimetry) chemical composition data, assuming simple additivity and taking the densities of polypyrrole, pristine tin(IV) oxide, and doped tin(IV) oxide to be 1.46, 4.77, and 4.34 g cm^{-3}, respectively. Standard deviations were calculated assuming normal statistics for the particle size distributions.

Morphology. Transmission electron microscopy (TEM) studies were made on dilute polypyrrole–tin(IV) oxide dispersions dried down onto carbon-coated copper grids (3 mm diameter, Agar Scientific Ltd.) using a Hitachi H-7100 instrument.

Surface Composition Studies. The surface composition of one of the polypyrrole–tin(IV) oxide nanocomposites was characterized using X-ray photoelectron spectroscopy (XPS) using a JEOL JPS-80 photoelectron spectrometer. The samples were prepared as follows; a ca. 5 × 5 mm piece of double-sided adhesive tape was used to stick a ca. 10 × 10 mm piece of Sellotape to the sample stub with the Sellotape being the adhesive side up. A microspatula tipful of the sample was then deposited in the center of the Sellotape and pressed down gently. Any loose material was carefully removed using an air duster. A separate control experiment was carried out to confirm that the Sellotape was purely hydrocarbon-based and contained no tin- or silicon-based contaminants which might otherwise affect the results. The sample analysis area was a circle of approximately 6.0 mm diameter.

Results and Discussion

In earlier papers we reported the synthesis of polypyrrole–silica nanocomposites using either $FeCl_3$ or $(NH_4)_2S_2O_8$ oxidants to polymerize pyrrole in the presence of ultrafine silica particles.[26,27] In contrast, in the present study we find that only $FeCl_3$ can be used for the preparation of stable colloidal dispersions of polypyrrole–tin(IV) oxide nanocomposites (see Table 1). Use of the $(NH_4)_2S_2O_8$ oxidant always led to macroscopic precipitation, with little or no colloidal formation. This observation may be related to the well-known kinetic differences between these two oxidants: Bjorklund has reported that the rate of polymerization of pyrrole is much faster with the $(NH_4)_2S_2O_8$ oxidant than the $FeCl_3$ oxidant.[32] However, it is possible that more subtle effects, such as the preadsorption of the reagents onto the surface of the inorganic oxide particles, may also play an important role in successful colloid formation.[27a]

In contrast to the silica and both the pristine and antimony-doped tin(IV) oxide particles, the zirconia, antimony(V) oxide, yttria, and titanium(IV) oxide dispersions do not appear to be effective dispersants, even

(31) Holsworth, R. M.; Provder, T.; Stansbrey, J. J. In *Particle Size Distribution*; Provder, T., Ed.; ACS Symp. Ser. No. 332; American Chemical Society: Washington, DC, 1987; Chapter 13, p 191.

(32) Bjorklund, R. B. *J. Chem. Soc., Faraday Trans. 1* **1987**, *83*, 1507.

Table 2. Effect of Tin(IV) Oxide Type and Initial Concentration on the Colloid Formation, Polypyrrole Content, Average Particle Size, and Conductivity of the Polypyrrole–Tin(IV) Oxide Nanocomposite Colloids

sample no.	tin(IV) oxide type[a]	initial tin(IV) oxide concn (w/v %)	colloid formation ?	polypyrrole content[b] (wt %)	particle size[c] (nm)	pellet conductivity (S cm^{-1})
1		0.0	no	100		8
2	SnO_2	1.0	no	74.8		2
3	SnO_2	1.3	partially	68.5		0.9
4	SnO_2	1.4	yes	63.4	550 ± 160	0.9
5	SnO_2	3.4	yes	39.8	340 ± 110	0.6
6[d]		0.0	no	100		34
7[d]	SnO_2	1.4	yes	71.1	470 ± 200	23
8	A-SnO_2	1.4	partially	62.0		7
9	A-SnO_2	1.5	yes	61.2	310 ± 160	4
10	A-SnO_2	1.8	yes	57.8	270 ± 80	7
11	A-SnO_2	3.4	yes	39.2	200 ± 50	4
12[d]	A-SnO_2	1.8	yes	30.4	260 ± 80	4

[a] "SnO_2" denotes the pristine tin(IV) oxide sol and "A-SnO_2" denotes the antimony-doped tin(IV) oxide sol. [b] As determined by elemental microanalysis (confirmed by thermogravimetry). [c] Weight-average diameter as determined by disk centrifuge photosedimentometry in pH 3 buffer solution. [d] In the presence of sodium *p*-tosylate.

at relatively high initial concentrations (up to 10 w/v %; see Table 1). These observations suggest that a high surface area colloidal substrate for the precipitating polypyrrole is a necessary, but not sufficient, condition for successful nanocomposite syntheses. On the other hand, the successful use of the tin(IV) oxide particles suggests that the formation of stable colloidal nanocomposites does not depend on some unique aspect(s) of the surface chemistry of silica. We note that silicon and tin are in the same group of the periodic table. Thus similarities in the surface chemistry of silica and tin(IV) oxide probably account for the observed effectiveness of these two sols as particulate dispersants for polypyrrole.

A summary of our experimental data on the synthesis, chemical composition, particle size, and conductivity of the polypyrrole–tin(IV) oxide nanocomposites is presented in Table 2. In the case of the pristine tin(IV) oxide sol, we note that a higher initial inorganic oxide concentration (1.4 wt %) is required for the quantitative formation of stable polypyrrole–tin(IV) oxide nanocomposite colloids compared to that required for polypyrrole–silica nanocomposite colloids (1.0 wt %).[26,27] An even higher initial concentration (1.5 wt %) is necessary for colloid formation with the antimony-doped tin(IV) oxide sol. The BET specific surface areas for the pristine tin(IV) oxide, antimony-doped tin(IV) oxide and silica samples were 129, 112, and 165 m^2 g^{-1}, respectively, while their corresponding densities (as measured by helium pycnometry) were 4.77, 4.34, and 2.17 g cm^{-3}. Using these combined BET and density, data, we calculate average particle diameters of 10 nm for the pristine tin(IV) oxide, 12 nm for the doped tin(IV) oxide and 17 nm for the silica. These values are in reasonably good agreement with our TEM observations (see Table 1). Furthermore, the minimum initial concentrations of pristin tin(IV) oxide, doped tin(IV) oxide, and silica sols required for successful nanocomposite formation correspond to total colloidal substrate surface areas of approximately 180, 168, and 165 m^2, respectively. Thus we conclude that, within experimental error, the two tin(IV) oxide sols have essentially the same dispersant efficiency as the silica particles. When comparing the performance of different particulate dispersants, it is clearly desirable to calculate the total surface area available in each synthesis rather than simply stating the intial concentration of the oxide particles. We wish to emphasise that the total surface area significantly exceeded 200 m^2 in the higher sol concentration syntheses utilised for each of the four "failed" inorganic oxides (see Table 1). Thus the failure of the yttria-, zirconia-, titania-, and antimony(V) oxide-based nanocomposite syntheses cannot be attributed to an insufficient amount of substrate surface area.

In our earlier papers the polypyrrole–silica nanocomposites were synthesized by adding the pyrrole monomer last to a stirred solution containing the chemical oxidant and the silica particles.[26,27] In the present study we have added an aqueous solution of the oxidant last to a stirred solution containing the pyrrole monomer and the inorganic oxide particles in all of our syntheses. In one of our recent studies (involving the copolymerization of pyrrole with a functionalized pyrrole monomer[28] we observed that such subtle differences were crucial to the success or failure of the colloid synthesis. Although not discussed in detail here we note that, for the homopolymerization of pyrrole in the presence of tin(IV) oxide or silica particles, the order of addition of the oxidant and the monomer does *not* appear to affect nanocomposite formation.

The conducting polymer content of the polypyrrole–tin(IV) oxide nanocomposites is influenced by the initial concentration of the inorganic oxide particles, with rather lower levels of polypyrrole being obtained at higher tin(IV) oxide concentrations (see Table 2; compare sample 4 with 5 and sample 9 with 11). We have previously reported similar observations for a wide range of polypyrrole–silica nanocomposite colloids prepared with both the $(NH_4)_2S_2O_8$ and $FeCl_3$ oxidants.[27] When calculating such conducting polymer contents we found that our thermogravimetric analyses were generally in good agreement with the corresponding microanalytical data. Using this chemical composition data, taking the tin(IV) oxide density data obtained by helium pycnometry and assuming both additivity and the density of bulk polypyrrole to be 1.46 g cm^{-3}, we calculate nanocomposite particle densities in the range 2.58–3.50 g cm^{-3} for samples 4, 5, 7, and 9–12. These values are significantly higher than those calculated for our polypyrrole-silica nanocomposites (typically 1.60 to 1.90 g cm^{-3}).

Our F.T.I.R. spectroscopy studies yielded useful, albeit qualitative, information on the polypyrrole–tin(IV) oxide nanocomposites. The spectrum of a sample of dried pristine tin(IV) oxide colloid (see Figure 2a) had one major band at 619 cm^{-1} and a weaker feature at

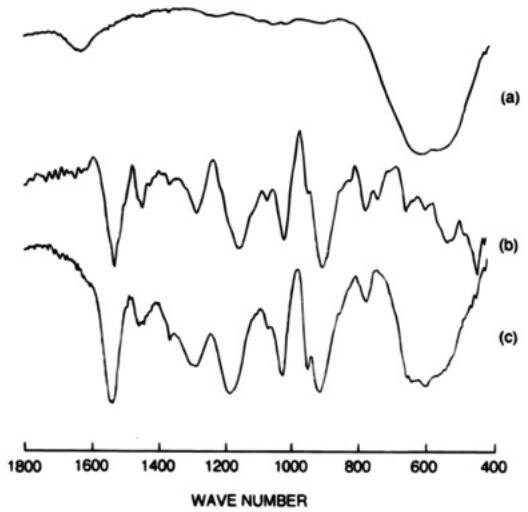

Figure 2. F.T.I.R. spectra (transmittance mode) of (a) pristine tin(IV) oxide; (b) polypyrrole bulk powder; (c) polypyrrole–tin(IV) oxide nanocomposite (sample 5).

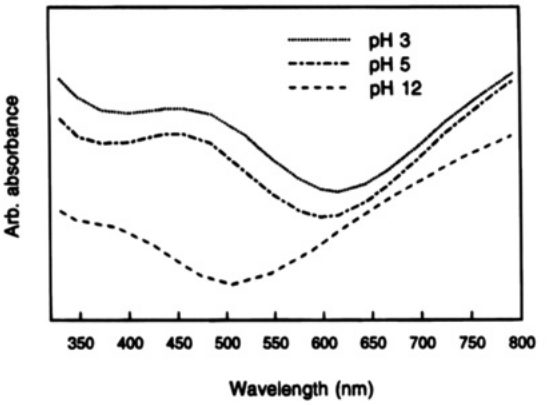

Figure 3. Visible absorption spectra of a polypyrrole–tin(IV) oxide nanocomposite colloid (sample 5) dispersed in pH 3, 5, and 12 buffer solutions.

1638 cm^{-1} in the 400–1800 cm^{-1} range. The F.T.I.R. spectrum of our polypyrrole bulk powder (sample 1) prepared with the $FeCl_3$ oxidant (see Figure 2b) confirmed the formation of doped polypyrrole with five bands at 1545, 1463, 1302, 1178, 1040, and 924 cm^{-1}.[9] As expected, the spectrum of the polypyrrole–tin(IV) oxide nanocomposites (see Figure 2c) clearly exhibited absorption bands attributable to both the polypyrrole (1533, 1475, 1306, 1205, 1046, and 934 cm^{-1}) and pristine tin(IV) oxide components (611 and 1638 cm^{-1}, although this latter feature is relatively weak). On the other hand, with our polypyrrole–silica nanocomposites we found that an intense broad absorption peak due to the silica component at around 1100 cm^{-1} tended to obscure several polypyrrole absorption bands.[27] Thus, the relatively featureless "window" in the F.T.I.R. spectrum of the pristine tin(IV) oxide sol in the 850–1600 cm^{-1} range affords a much easier examination of the absorption bands due to the conducting polymer component.

The visible absorption spectra of polypyrrole–tin(IV) oxide diluted in buffer solutions in the pH range 3–12 are shown in Figure 3. This technique "sees" only the polypyrrole component since the original pristine tin(IV) oxide sol is almost transparent (N.B. the doped tin(IV) oxide sol is orange-brown, presumably due to the mixed-valence antimony species). Our spectra are similar to those reported by Pei and Qian for polypyrrole films soaked in various buffer solutions.[33] The absorption band at around 450 nm exhibited by polypyrrole in acidic media shifts to around 380 nm in basic media. Unfortunately we were not able to follow any shifts in the absorption peak centered at ca. 950 nm[9,33] since this spectral region was beyond the range of our spectrophotometer. We note that at pH 12 the N–H groups of the polypyrrole component should be extensively deprotonated,[33,34] resulting in a reduction in the number of mobile charge carriers on the conjugated polymer backbone. Thus a substantial loss in electrical conductivity of several orders of magnitude occurs.[33] This effect has been reported to be almost completely reversible for electrochemically synthesized polypyrrole films: addition of acid to the solution causes reprotonation of the nitrogen atoms on the polypyrrole chains and a concomitant increase in conductivity back to near to the original value.[34]

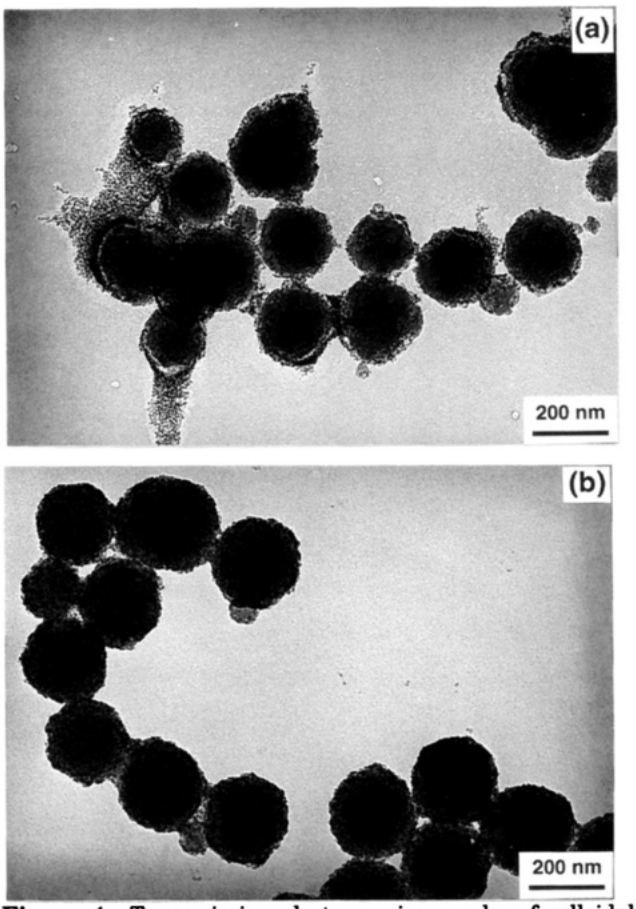

Figure 4. Transmission electron micrographs of colloidal nanocomposites of polypyrrole–tin(IV) oxide synthesized using (a) the pristine tin(IV) oxide sol (sample 5 in Table 2) and (b) the antimony-doped tin(IV) oxide sol (sample 11 in Table 2).

Transmission electron micrographs of diluted polypyrrole–tin(IV) oxide dispersions synthesized using the pristine and doped tin(IV) oxide sols are shown in Figures 4a (sample 5) and 4b (sample 11), respectively. In both cases the nanocomposite particles are rather polydisperse, with size ranges of 140–320 and 160–300 nm, respectively. The individual tin(IV) oxide particles

(33) Pei, Q.; Qian, R. *Synth. Met.* **1991**, *45*, 35.
(34) (a) Inganas, O.; Erlandsson, R.; Nylander, C.; Lundstrom, I. *J. Phys. Chem. Solids* **1984**, *45*, 427. (b) Münstedt, H. *Polymer* **1986**, *27*, 899.

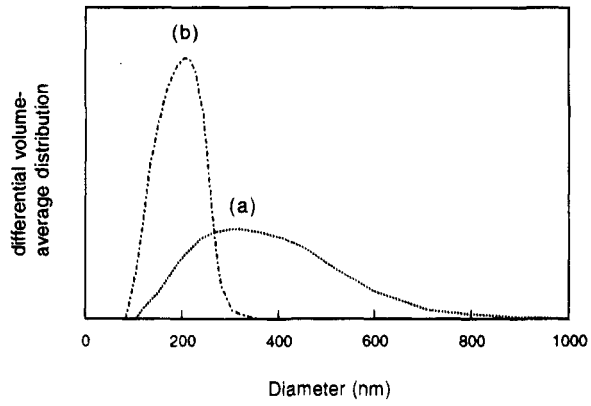

Figure 5. Weight-average particle size distribution curves of polypyrrole-tin(IV) oxide nanocomposite particles obtained using the disk centrifuge: (a) sample 5, (b) sample 11.

within these nanocomposites are clearly visible and give rise to a "raspberry"-like morphology. We note that even our best polypyrrole–tin(IV) oxide sample (sample 11) seems to be significantly more polydisperse than the relatively monodisperse polypyrrole-silica nanocomposites reported earlier (see our disc centrifuge data below).[26,27]

Typical weight-average particle size distribution curves of the polypyrrole–tin(IV) oxide nanocomposites (samples 5 and 11) obtained using our disk centrifuge instrument are shown in Figure 5. This particle sizing technique confirms our qualitative electron microscopy observations. For example, polypyrrole–tin(IV) oxide sample 5 has a polydispersity (D_w/D_n) of 1.39 (and a weight-average diameter D_w of 340 ± 110 nm), while most of our polypyrrole–silica nanocomposite samples exhibited rather lower polydispersities (typically in the range 1.10–1.20). The particle size distributions of the polypyrrole–tin(IV) oxide nanocomposites are clearly influenced by the initial pristine (or doped) tin(IV) oxide concentration, with rather larger particles and broader size distributions being obtained at lower tin(IV) oxide concentrations (see Table 2). We have reported similar observations for polypyrrole-silica nanocomposites prepared with both the $(NH_4)_2S_2O_8$ and $FeCl_3$ oxidant.[27] Considering this TEM and DCP particle size data together with our conclusions from a recent small-angle X-ray scattering (SAXS) study on a polyaniline–silica nanocomposite,[35] it is clear that the polypyrrole nanomorphology within a polypyrrole–tin(IV) oxide particle must be *substantially different* to the morphology of the large globular, fused particulates (dimensions of the order of 200–500 nm) which are commonly observed in conventional polypyrrole bulk powder.[27a]

We decided to study the surface composition of a polypyrrole–tin(IV) oxide nanocomposite sample in order to gain some insight into the colloid stability mechanism of these dispersions. Thus, the surface composition of sample 5 was examined by X-ray photoelectron spectroscopy (XPS), a well-established and highly surface-specific technique (the typical sampling depth is 2–10 nm). The bulk composition of this nanocomposite was determined from our thermogravimetry and elemental microanalysis macroscopic data. In our XPS experiment we utilised the tin atoms in the

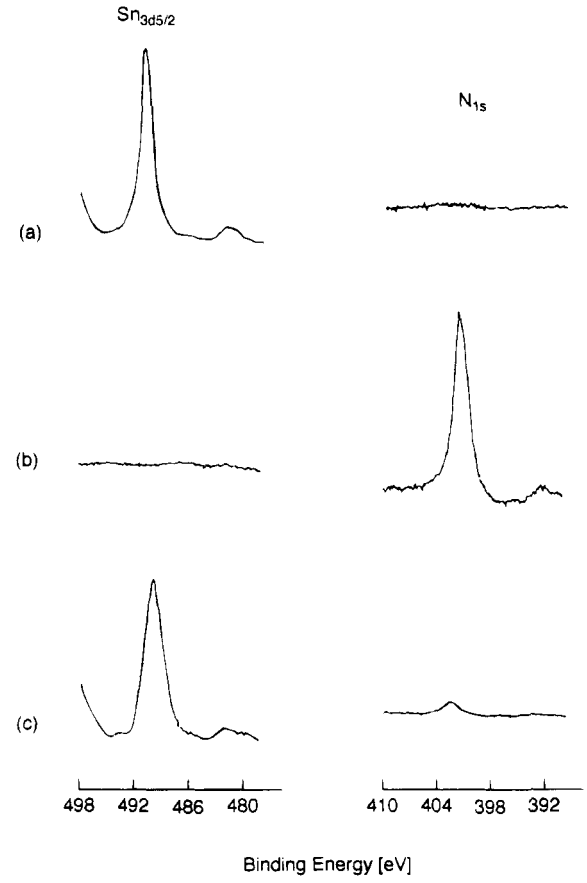

Figure 6. Typical wide scan survey XPS spectra of (a) bare tin(IV) oxide; (b) polypyrrole bulk powder; (c) polypyrrole–tin(IV) oxide nanocomposite (sample 5).

tin(IV) oxide component and the nitrogen atoms in the polypyrrole component as elemental "markers". Since these "markers" are unique for each component (see Figure 6a,b), simply measuring the tin/nitrogen atom ratios by XPS enabled us to make a semi-quantitative assessment of the tin(IV) oxide/polypyrrole surface composition of the nanocomposites (with the tin elemental marker we arbitrarily decided to utilize only the area of $Sn_{3d5/2}$ peak, rather than the total area of the eight Sn peaks, for comparison with the N_{1s} peak area; the $Sn_{3d5/2}$ peak area was adjusted using well-documented sensitivity factors so as to determine the actual surface concentration of tin atoms).[36] These surface atomic ratios were then compared with the bulk tin/nitrogen atomic ratios of the nanocomposites calculated from our macroscopic chemical composition data. For example, in sample 5, the *surface* tin/nitrogen ratio was found to be 17.2 (see Figure 6c), whilst the *bulk* tin/nitrogen was calculated to be 0.3. The experimental errors associated with these two tin/nitrogen atomic ratios are estimated to be 10% and 10–15% respectively. Thus the observed difference is well outside experimental error. We conclude that, although the presence of a N_{1s} signal confirms the presence of polypyrrole at the surface of the polypyrrole–tin(IV) oxide particles (see Figure 6c; N_{1s} spectrum), the conducting polymer is substantially depleted from the surface of these nanocomposites.

(35) Terrill, N. J.; Crowley, T.; Gill, M.; Armes, S. P. *Langmuir* **1993**, *9*, 2093.

(36) Moulder, J. F.; Stickle, W. F.; Sobol, P. E.; Bomben, K. D. In *Handbook of X-ray Photoelectron Spectroscopy*; Chastain, J., Ed.; Perkin-Elmer Corp.: Physical Electronics Division, Eden Prairie, MN, 1992; p 25.

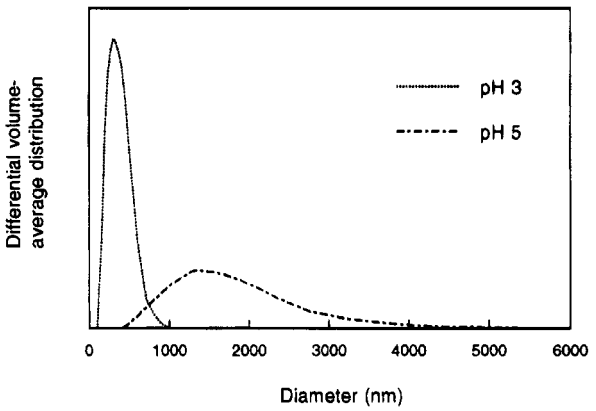

Figure 7. Weight-average particle size distribution curves of polypyrrole–tin(IV) oxide nanocomposite particles (sample 5) dispersed in pH 3 and pH 5 buffer solutions obtained using the disk centrifuge.

Thus, in the context of colloidal stability, the polypyrrole–tin(IV) oxide nanocomposite particles can, to a first approximation, be considered simply as "large" tin(IV) oxide particles, i.e., they are probably charge-stabilized like the original small tin(IV) oxide particles. We have made similar observations on a wide range of polypyrrole-silica nanocomposite colloids (i.e., that such dispersions have distinctly silica-rich surfaces) which will be reported in detail elsewhere.[37]

The disk centrifuge is a useful instrument for assessing the degree of dispersion of the nanocomposite particles over a range of solution pH. In these experiments a shift in the weight-average particle size distribution to higher particle diameter indicates an increase in the degree of flocculation of the dispersion, rather than an actual increase in particle diameter. Our results are depicted in Figure 7. One of our polypyrrole–tin(IV) oxide nanocomposites (sample 5) is reasonably stable in a pH 3 buffer solution; it is therefore more stable with respect to pH-induced flocculation than our earlier polyaniline–silica dispersions which were quantitatively flocculated under these conditions.[38] On the other hand, the same polypyrrole–tin(IV) oxide sample is immediately flocculated upon addition to a pH 5 buffer solution. Thus such dispersions are certainly not as stable to aggregation as the polypyrrole–silica nanocomposite dispersions, which remained stable even in pH 9 buffer solutions.[37] We note that, at pH 5, the polypyrrole–tin(IV) oxide particles are electrically conductive but flocculated, whereas the polypyrrole–silica particles in the pH 9 buffer are dispersed but probably somewhat less conductive due to deprotonation of the polypyrrole chains.[33] The poor colloid stability of the polypyrrole–tin(IV) oxide nanocomposites at physiological pH is likely to prevent their use as "marker" particles in diagnostics assays (a potential application which we are currently evaluating for the more stable polypyrrole–silica particles).

In general, we note that all of the polypyrrole–tin(IV) oxide nanocomposites have higher solid-state conductivities than the corresponding polypyrrole–silica nanocomposites. For example, despite its lower polypyrrole content, polypyrrole–tin(IV) oxide sample 5 (polypyrrole content 38 wt %) exhibited slightly higher conductivity than our earlier polypyrrole–silica nanocomposite samples (polypyrrole content 61–71 wt %).[27] Since our XPS studies suggest that the conducting polymer is somewhat depleted from the surface of the nanocomposite particles, these conductivity values most likely reflect the substantial difference in conductivity between the semiconducting tin(IV) oxide particles and the electrically insulating silica particles [we measured the compressed pellet conductivities of pristine and doped tin(IV) oxide to be 2.0×10^{-3} and 7.6×10^{-2} S cm^{-1}, respectively, whereas the conductivity of silica ($<10^{-6}$ S cm^{-1}) was too low to be measured with our four-point probe apparatus]. Indeed, use of the more conductive antimony-doped tin(IV) oxide yielded polypyrrole–tin(IV) oxide nanocomposites with conductivities as high as 7 S cm^{-1} (see Table 2, samples 9–11). On the other hand, since the conductivities of samples 4 and 5 were both significantly higher than tin(IV) oxide alone, the polypyrrole component must also make a contribution to the interparticle conductivity mechanism. To test this hypothesis and also to obtain higher conductivities, we synthesized a polypyrrole–tin(IV) oxide nanocomposite in the presence of sodium *p*-tosylate (sample 7). It is well-known that this approach yields *p*-tosylate-doped polypyrrole, which is approximately an order of magnitude more conductive than sulfate- or chloride-doped polypyrrole.[27a] As anticipated, we observed a similar enhancement in conductivity up to 23 S cm^{-1} for a *p*-tosylate-doped polypyrrole–tin(IV) oxide nanocomposite synthesized using the pristine tin(IV) oxide sol (see sample 7). Surprisingly, addition of sodium *p*-tosylate to nanocomposite syntheses utilizing the antimony-doped tin(IV) oxide sol did *not* result in any improvement in conductivity (compare samples 9 and 11). We have no explanation for this apparent anomaly at the present time.

Conclusions

We have attempted to extend our earlier syntheses of polypyrrole–silica nanocomposites by chemically polymerizing pyrrole in the presence of titania, yttria, zirconia, tin(IV) oxide, and antimony(V) oxide particles. Of these dispersions, we find that only the tin(IV) oxide sol acts as an effective particulate dispersant for the conducting polymer. Thus a high surface area colloidal substrate is a necessary but not sufficient condition for the formation of stable colloidal dispersions of polypyrrole–inorganic oxide nanocomposite particles. It is possible that there is some specific, and as yet unidentified, aspect(s) of the surface chemistry of the silica and tin(IV) oxide particles which promotes nanocomposite formation. We note that, under the particular conditions utilized for our polypyrrole syntheses, the silica, pristine tin(IV) oxide and doped tin(IV) oxide particles require very similar minimum substrate surface areas (165, 180, and 168 m^2, respectively) for successful colloid formation.

Both the conducting polymer content and particle size of the polypyrrole–tin(IV) oxide nanocomposites are influenced by the initial tin(IV) oxide concentration: lower polypyrrole contents and smaller, less polydisperse nanocomposite particles are obtained at higher tin(IV) oxide concentrations. Since the density of tin(IV) oxide is rather higher than that of silica, the

(37) Maeda, S.; Gill, M.; Armes, S. P.; Fletcher, I. W. Submitted to *Macromolecules*.
(38) Gill, M. Ph.D. Thesis, University of Sussex **1994**.

densities of the polypyrrole–tin(IV) oxide particles are significantly higher than the corresponding polypyrrole–silica system (2.58–3.50 g cm^{-3} vs 1.60–1.90 g cm^{-3}).

The surface composition of the polypyrrole–tin(IV) oxide nanocomposites is tin(IV) oxide-rich relative to their bulk composition. Since the polypyrrole component is somewhat depleted from the surface of the particles, the polypyrrole–tin(IV) oxide nanocomposite particles can, to a first approximation, be considered to be "large" charge-stabilized tin(IV) oxide particles. With respect to pH-induced flocculation, the polypyrrole–tin(IV) oxide nanocomposite particles are reasonably stable at pH 3 but flocculate at pH 5. Thus the polypyrrole–tin(IV) oxide particles are more resistant to pH-induced flocculation compared to polyaniline–silica colloids but rather less stable than the polypyrrole–silica colloids.

The solid-state compressed pellet conductivities of the polypyrrole–tin(IV) oxide nanocomposites are always appreciably higher than those of the polypyrrole–silica nanocomposites prepared under similar conditions. This is largely due to the relatively high intrinsic conductivity of tin(IV) oxide compared to silica. In addition, the conductivities of polypyrrole–tin(IV) oxide nanocomposites synthesized using the antimony-doped tin(IV) oxide sol are approximately an order of magnitude higher than those synthesized with the pristine tin(IV) oxide sol. The use of sodium *p*-tosylate in the colloid syntheses can produce nanocomposites with conductivities as high as 23 S cm^{-1}. Like the polypyrrole–silica nanocomposites, the polypyrrole–tin(IV) oxide system represents a potentially useful processable form of polypyrrole, a normally intractable conducting polymer.

Acknowledgment. We acknowledge Dr. T. Swank and Dr. D. Catone of Nyacol Products, Inc., and Dr. B. Meldrum of Tioxide Specialities Ltd. for the generous donation of the various inorganic oxide sols. Micromeritics (U.K.) Ltd. and QuantaChrome (U.K.) Ltd. are also gratefully acknowledged for the loan of their helium pycnometers and BET instruments. The SERC is acknowledged for two capital equipment grants for the purchase of the disk centrifuge photosedimentometer and thermogravimetric analyzer (GR/H93606 and GR/F73977 respectively). Finally, S.M. thanks the New Oji Paper Co. Ltd. for generous financial support in the form of a Ph.D. studentship.